
Article:
Rozhnoi, A., Shalimov, S., Solovieva, M. et al. (6 more authors) (2014) Detection of tsunami-driven phase and amplitude perturbations of subionospheric VLF signals following the 2010 Chile earthquake. Journal of Geophysical Research: Space Physics, 119 (6). pp. 5012-5019. ISSN 2169-9380

https://doi.org/10.1002/2014JA019766

AGU PUBLICATIONS

JGR

Journal of Geophysical Research: Space Physics

RESEARCH ARTICLE
10.1002/2014JA019766

Key Point:
- Chile tsunami detected by VLF signal and confirmed by DART data

Correspondence to:
A. Rozhnoi,
rozhnoi@ifz.ru

Citation:
Rozhnoi, A., S. Shalimov, M. Solovieva, B. Levin, G. Shevchenko, M. Hayakawa, Y. Hobara, S. N. Walker, and V. Fedun (2014), Detection of tsunami-driven phase and amplitude perturbations of subionospheric VLF signals following the 2010 Chile earthquake, *J. Geophys. Res. Space Physics*, *119*, 5012–5019, doi:10.1002/2014JA019766.

Received 7 JAN 2014
Accepted 29 MAY 2014
Accepted article online 2 JUN 2014
Published online 16 JUN 2014

Detection of tsunami-driven phase and amplitude perturbations of subionospheric VLF signals following the 2010 Chile earthquake

A. Rozhnoi[1], S. Shalimov[1,2], M. Solovieva[1], B. Levin[3], G. Shevchenko[3], M. Hayakawa[4], Y. Hobara[4], S. N. Walker[5], and V. Fedun[5]

[1]Institute of the Earth Physics, RAS, Moscow, Russia, [2]Space Research Institute, RAS, Moscow, Russia, [3]Institute of Marine Geology and Geophysics, FEB RAS, Yuzhno-Sakhalinsk, Russia, [4]Department of Communication Engineering and Informatics, University of Electro-Communications, Advanced Wireless Communications Research Center, Chofu, Japan, [5]Department of Automatic Control and Systems Engineering, University of Sheffield, Sheffield, UK

Abstract We report on specific fluctuations in phase and amplitude of VLF signals that correlate both spatially and temporally with the passage of the tsunamis recorded by the Deep-ocean Assessments and Reporting of Tsunamis bottom pressure stations. Measurements from the VLF/LF receiver sited in Petropavlovsk-Kamchatsky and sensor buoys placed throughout the Pacific Ocean at great distances (Hawaii and Japan) from the epicenter are consistent with the hypothesis that the ocean tsunami following the Chile earthquake on 27 February 2010 radiated internal gravity waves which propagated through the lower ionosphere.

1. Introduction

In the last decade the ionospheric response caused by the passage of tsunami has been firmly established. Such a connection was proposed in the 1970s [*Hines*, 1972; *Najita et al*., 1974; *Peltier and Hines*, 1976] as the basis for the early detection of tsunami. Numerical modeling demonstrated that the ionospheric signature of an ocean tsunami can potentially be detected in the upper ionosphere as traveling ionospheric disturbances (TIDs) produced by internal gravity waves propagating through the atmosphere [e.g., *Occhipinti et al*., 2006, 2008; *Hickey et al*., 2009; *Mai and Kiang*, 2009]. Evidence for tsunami-driven TIDs has been observed in measurements of the ionospheric total electron content (TEC) using ground-based GPS radio signals [e.g., *Artru et al*., 2005; *Rolland et al*., 2010] and satellite-based altimeter radar [*Occhipinti et al*., 2006].

These observations were attributed to the response of the upper ionosphere (*F* region) to the arrival of internal gravity waves initiated by the passage of a tsunami. The possibility of a new ground-based technique (over-the-horizon radars), for tsunami detection through ionospheric monitoring (*E* region), has been suggested and simulated [*Coïsson et al*., 2011]. Recently, the response of the lower ionosphere has been experimentally investigated by *Rozhnoi et al*. [2012] based on measurements of the propagation of subionospheric VLF following the Kuril 2006 and Tohoku 2011 earthquakes. These authors reported perturbations both in the phase and in amplitude of VLF signal that began about 1.5 h after the earthquakes occurred and continued while the tsunamis propagated within the sensitivity zone of the propagation path between the transmitter and receiver. A qualitative interpretation of the observed effects has been suggested in terms of the interaction of internal gravity waves with lower ionosphere.

In the present study we use phase and amplitude observations of subionospheric VLF signals to analyze the response of the lower ionosphere following the tsunamigenic Chilean 2010 earthquake from 26 to 32 h after the earthquake when the corresponding tsunami reached the sensitivity zone between the transmitter and receiver.

It should be noted that *Galvan et al*. [2011] reported evidence of variations in GPS TEC measurements that were associated with the tsunami observed on 27 February 2010 following the Chilean earthquake. These authors detected the tsunami-driven internal gravity waves in the form of TIDs at locations in Hawaii and Japan. Using DARTs (Deep-ocean Assessments and Reporting of Tsunamis) sensor buoy measurements from Hawaii and Japan, we show that after this earthquake there observed two temporally well-separated tsunami events, the second of which produces the most pronounced amplitude and phase perturbations of VLF signals.

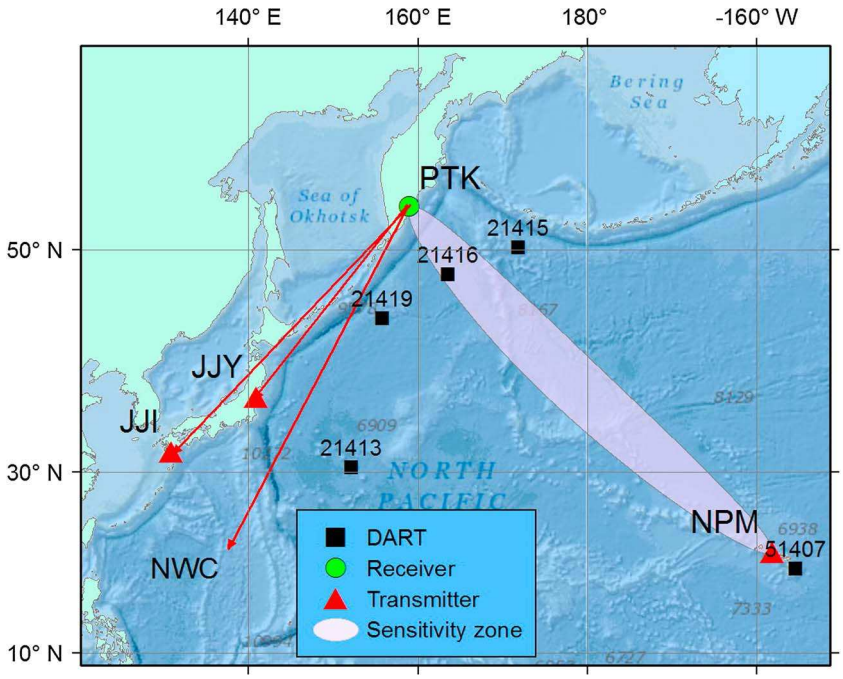

Figure 1. A map showing the position of the receiver in Petropavlovsk-Kamchatsky (PTK) and the transmitter NPM (21.4 kHz), JJI (22.2 kHz), and JJY (40 kHz) together with the position of the deep water DART stations in the region under analysis. The pink ellipse is projection of the fifth Fresnel sensitivity zone on the Earth's surface. The direction to the NWC (19.8 kHz) transmitter in Australia is shown by red arrow.

2. Results of Analysis

The analysis reported in this paper is based on the data recorded by the VLF ground-based station in Petropavlovsk-Kamchatsky (PTK), Russia. The receiver simultaneously measures the amplitude and phase of signals from the transmitters located in Japan (JJY and JJI), Australia (NWC), and Hawaiian Islands (NPM) with a time resolution of 20 s. For the analysis of the VLF signal variations observed after the earthquake the subionospheric path Hawaii-Petropavlovsk-Kamchatsky (NPM-PTK) was used because it extends along the propagation direction of the tsunami. The other propagation paths were used as the control group. These measurements are compared with those from the Deep-ocean Assessments and Reporting of Tsunamis (DARTs) bottom pressure stations operated by the United States National Oceanic and Atmospheric Administration (NOAA). DART buoys record seafloor pressure with sampling 15 s; then data are averaged over 15 min interval and transmitted every hour via satellite to the U.S. National Data Buoy Center which manages and conducts all operational network activities and distributes real-time data to the public. In case of a tsunami event, buoys begin to transmit the 15 s data directly during several minutes before the buoy switches to 1 min averages until the end of the event mode. The 15 s data are stored in the instrument package and downloaded following instrument retrieval [*Mungov et al.*, 2013]. In present study we use these retrieved 15 s data.

Figure 1 shows the position the NPM-PTK path together with the location of the DART stations in the northern Pacific region. Data recorded by DART sensors 51407 and 21416 were used in the analysis because they are located at each end of the VLF propagation path under consideration. The ellipse shows the sensitivity zone which corresponds to the fifth Fresnel zone.

A strong earthquake with magnitude $M_w = 8.8$ occurred on 27 February 2010, at 06:34 UT near the Central Chilean coast. The epicenter of the main shock, as recorded by the U.S. Geological Survey, was located at 35.846°S and 72.719°W with a focal depth of 35 km. This earthquake caused a destructive tsunami that resulted in severe damage along the coast of Chile and presented a serious threat to all Pacific Ocean coastal regions including the far eastern coast of Russia. This tsunami was recorded throughout the Pacific Ocean (http://wcatwc.arh.noaa.gov/previous.events/?p=Chile_02-27-10). The tsunami propagation time from its source to the Hawaiian Islands was about 14 h, and then, 7 h later it reached the coast of Russia.

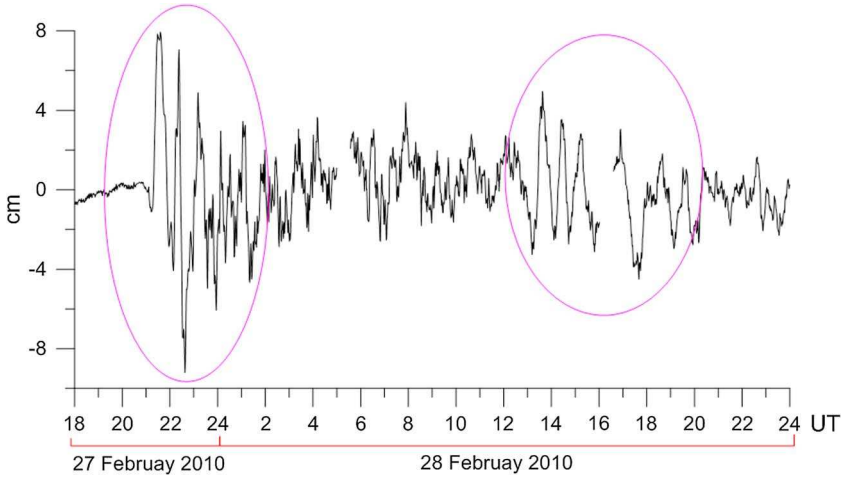

Figure 2. The record of the Chilean tsunami of 27–28 February 2010 by DART station 51407 located near Hawaii Islands. The ellipses highlight the arrival of the first and second waves.

The tsunami produced a long-lasting ocean surface perturbation which is typical for strong transoceanic tsunamis. Studies of tsunami decay are performed in many publications [e.g., *Van Dorn*, 1984, 1987; *Rabinovich et al*., 2011] based on coastal measurements. The development of DART stations distributed throughout the entire Pacific Ocean enables to obtain more precise information on decay times. Open ocean energy decay of the 2009 Samoa, 2010 Chile, and 2011 Tohoku tsunamis in time and space was investigated by *Rabinovich et al*. [2013] based on large number of DART stations in the Pacific Ocean. The mean decay time for the Chile tsunami for the 23 DART records was found to be 24.7 h. Detailed analysis of the Sumatra tsunami and numerical modeling of tsunami propagation in an ocean was produced by *Levin and Nosov* [2009]. Numerical modeling supported by observational data shows that two main factors influence on tsunami propagation. It is the geometry of the source in the near-field zone, and it is the topography of the ocean floor in the far-field zone. In the far zones the maximum of tsunami amplitude can be observed with delay from several to 24 h after arrival of the lead wave due to reflections from coasts and underwater obstacles and propagation along natural waveguide-underwater ridges.

Figure 2 shows the oscillations of the sea level recorded by DART sensor buoy 51407 located near Hawaii during 27–28 February. Two large disturbances can clearly be seen that occur at 21 UT on 27 February and 13 UT on 28 February. Both events are characterized by dominant low-frequency oscillations of the surface height. These two waves can also be clearly seen in the spectral-time diagrams (reconstructed following the methods by *Dziewonski et al*. [1969] and *Lander et al*. [1973]) of the sea level oscillations recorded by DART 51407 shown in Figure 3. The first wave exhibits intense spectral components in the range of 20–50 min followed by gradual decay away during 7–9 h. The periods of the second tsunami-like wave are in the range of 30–50 min.

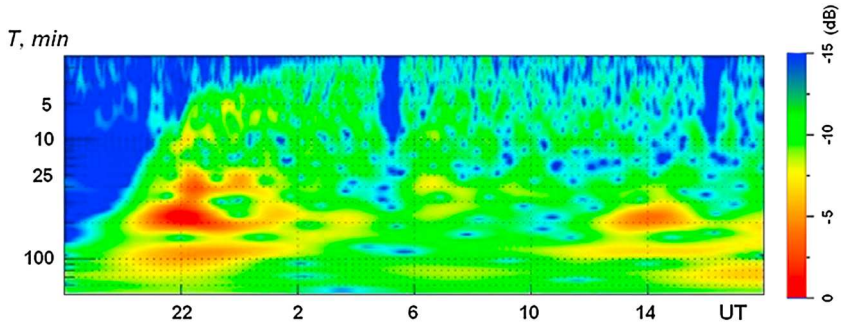

Figure 3. Spectral-time diagram of sea level oscillations recorded by DART 51407 for the period from 18:00 27 February to 18:00 28 February 2010. Axis *X* is time (UT). Axis *Y* is period.

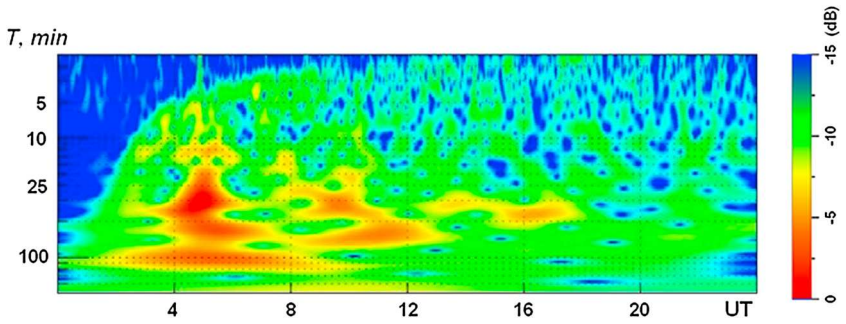

Figure 4. Spectral-time diagram of sea level oscillations recorded at DART 21416 on 28 February 2010. Axis *X* is time (UT). Axis *Y* is period.

More likely that this second major wave is a result of reflection off of Japan. This hypothesis is supported by NOAA's Method of Splitting Tsunami model (see the animation for the Chile tsunami: http://nctr.pmel.noaa.gov/chile20100227/20100227Chile.mov) and modeling made by Artem Loskutov (private report). This modeled behavior is consistent with the DART 51407 data presented in Figures 2 and 3.

Figure 4 shows the spectral-time diagram of sea level oscillations recorded by DART 21416 on 28 February 2010. It is clearly seen that intense sea level oscillations lasted at this station until the end of the day. The strongest oscillations, caused by the first tsunami arrival, were detected at about 3 UT. However, rather strong oscillations with alternating intensity occurring in the frequency range of 20–50 min can be noticeable up to the end of the interval 9–11 UT.

Figure 5 shows the phase and amplitude perturbations of the VLF signal (21.4 kHz) recorded along the NPM-PTK subionospheric path from the transmitter located in Hawaii on 27–28 February 2010 (blue line) together with the monthly averaged signal (red dotted line) that was calculated using data from undisturbed days. The VLF signal exhibits a diurnal effect with strong changes occurring during the periods of sunset and sunrise when the altitude of the lower ionosphere changes abruptly. The VLF signal reflects from the ionosphere in the night at the altitudes ~90 km and in the day at the altitudes ~70 km. The characteristics of the daytime lower ionosphere are determined primarily by solar activity. Therefore, the VLF signal is rather stable during the day period and unaffected by any other external factors (for example, even by magnetic storms [*Rozhnoi et al.*, 2006]). Therefore, nighttime observations provide the optimal conditions for the detection of ionospheric disturbances by the VLF signals. The green bar in Figure 5 marks the nighttime period at both sites (Hawaii and Petropavlovsk-Kamchatsky) and indicates the period of data that has been used in the subsequent analysis.

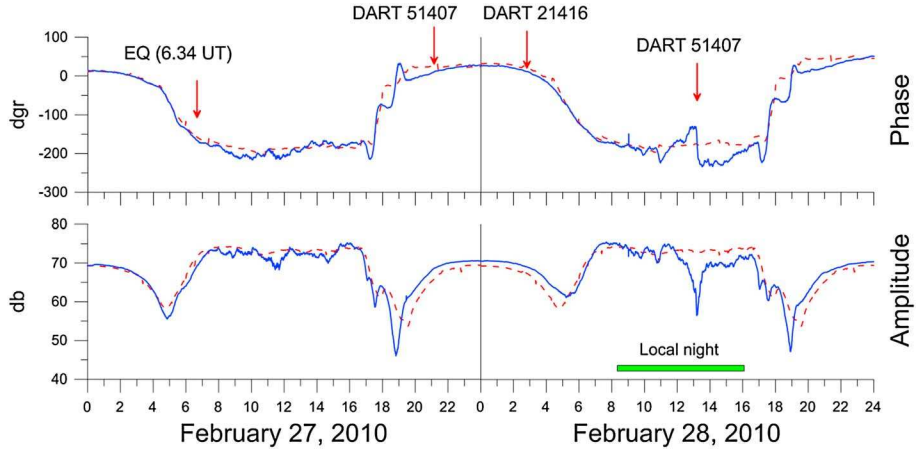

Figure 5. (top) Phase and (bottom) amplitude of the signal from NPM transmitter recorded in Petropavlovsk-Kamchatsky on 27–28 February 2010. Blue solid lines and red dotted lines are the observed and quiet time averaged signals, respectively. The arrows show the occurrence time of the earthquake on 27 February 2010, arrival of the tsunami to the DART 51407 on 27 February 2010, and at DART 21416 on 28 February 2010 as well as arrival of the second wave of the tsunami to the DART 51407 on 28 February 2010. The horizontal green rectangle in the bottom right indicates the local nighttime interval.

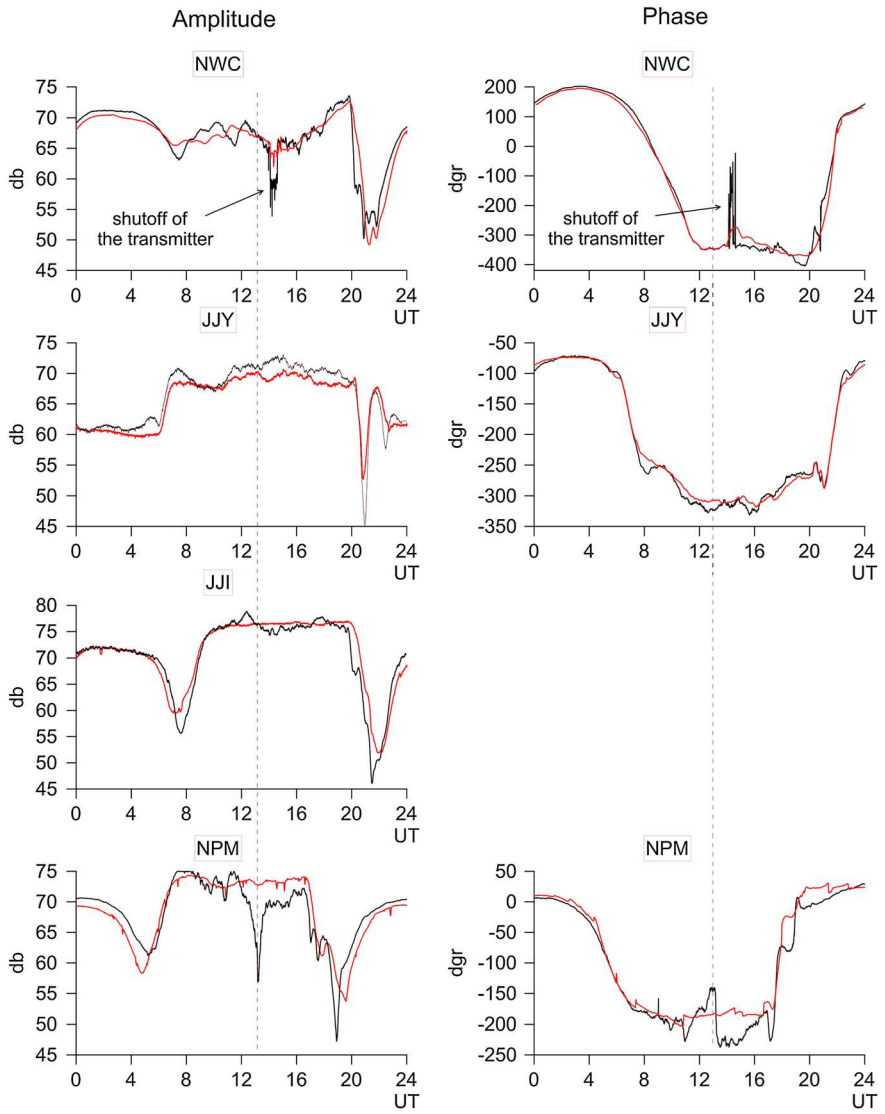

Figure 6. (left) Amplitude and (right) phase of the signals from four transmitters, NWC (19.8 kHz), JJY (40.0 kHz), JJI (22.2 kHz), and NPM (21.4 kHz), recorded in Petropavlovsk-Kamchatsky on 28 February 2010. Black and red lines are the observed and averaged signals, respectively. The dotted vertical line shows the arrival time of the second wave of tsunami on DART 51407.

Arrows in Figure 5 mark the occurrence time of the earthquake on 27 February 2010 and the subsequent arrival time of the tsunami at the DART buoys near the NPM-PTK subionospheric VLF path. The first or main tsunami was recorded by the buoy 51407 near Hawaii on 27 February 2010 at about 21 UT. This time corresponds to local daytime conditions so that any disturbance of the NPM-PTK VLF signal was not expected. This tsunami appeared at DART 21416 near Kamchatka on 28 February 2010 at around 3 UT, which also occurred during local daytime conditions. However, the second tsunami-like wave was recorded by DART 51407 on 28 February 2010 at around 13 UT during the local nighttime for the NPM-PTK subionospheric path.

The NPM-PTK signal recorded during the local nighttime period on 28 February shows noticeable decrease in amplitude (about 15 dB) together with phase variations (up to 40°) relative to the background (the monthly averaged signal) around the time when the second tsunami-like wave arrived at DART 51407 (Figure 5). This result strongly contrasted with those signals propagating along the other paths passing far away from Hawaii (JJY-PTK, JJI-PTK, and NWC-PTK) whose amplitude and phase do not deviate from monthly averaged signal (Figure 6). It should be noted that geomagnetic conditions on this day were extremely quiet (*Kp* ~ 0.7, *Dst* ~ 0–10 nT), and data from the geostationary satellite GOES showed no increase in the relativistic electron fluxes or proton bursts.

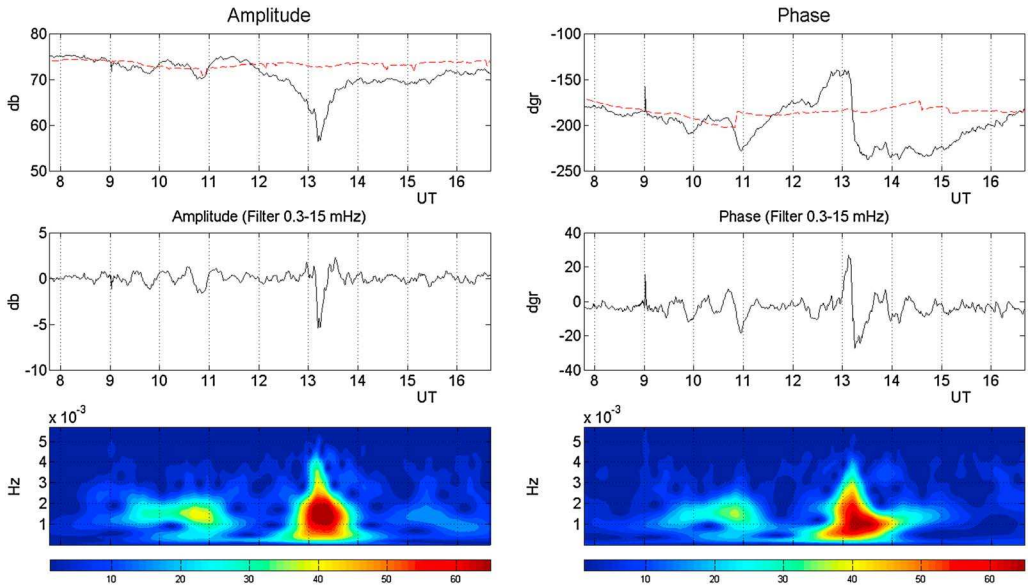

Figure 7. Top row shows (left) the amplitude and (right) the phase of the signal from the NPM transmitter recorded on 28 February 2010 in Petropavlovsk-Kamchatsky during local night. Dotted lines are the averaged signals. The middle row shows the signals filtered in the range 0.3–15 mHz. The bottom row shows the wavelet spectra of the filtered signals.

The maximum intensity of the observed anomaly in the VLF signal (see Figure 5) coincides with the arrival of the second tsunami-like wave at DART 51407 about 13 UT while changes in the signal began approximately 1 h earlier.

Though the largest perturbation in phase and amplitude began at around 12 UT (see Figure 5), the smaller amplitude and phase perturbations were observed from the beginning of the local nighttime period. These nighttime signals are shown in greater temporal detail in Figure 7. The panels show the complete waveform (top), the waveform filtered in the range 0.3–15 mHz (which correspond to periods from about 1 min to 60 min) (middle), and the wavelet spectrogram of the filtered signal (bottom) for the amplitude (left) and phase (right) of the VLF signal propagating along the NPM-PTK path during local nighttime conditions.

It can be seen from Figure 7 that the frequency of the maximum spectral amplitude is in the range of 0.5–2 mHz (i.e., periods of 10–50 min) which corresponds to the range of periods for internal gravity waves. These periods are also in agreement with the periods observed in data recorded by DART sensor buoys (see Figures 3 and 4). We suppose that the gravity waves interact with lower ionosphere during 9–11 UT when the first tsunami wave near Kamchatka is still active (see Figure 4). After that, approximately 1 h interval without perturbations follows which ends up at 12 UT and then perturbations develop again up to their maximum at 13 UT. This moment corresponds to the arrival of the reflected tsunami wave at Hawaiian Islands. We can suppose that observed perturbations in the VLF signal around 12 UT start to develop due to the reflected tsunami wave moving southeastward from Japan and passing through the VLF zone of sensitivity before arriving at the DART 51407 station around 13 UT.

3. Discussion and Conclusion

Our experimental results show that the upper boundary of the VLF waveguide has been perturbed most likely by tsunami-driven gravity waves that propagate through the lower ionosphere. In order to give a more qualitative interpretation, we develop a first-order analytical formulation of the problem following a simplified approach based on certain limiting assumptions. An example and details of such an approach has been demonstrated in our previous paper [*Rozhnoi et al*., 2012]. Here we only stress main points of the approach.

We have used two assumptions to simplify the analysis. The first one includes consideration of the "ground," consisting of sea water, as a perfect conductor, when the propagation of signals in the frequency range 10–25 kHz over a long all-sea path is analyzed. Our second assumption relates with a consideration of the lower ionosphere as a medium with either a sharp boundary or an exponential profile [*Wait*, 1959; *Wait and Spies*, 1964]. Assuming in addition that the ionospheric region perturbed by a tsunami-driven gravity wave is

distant (at least ~200–500 km) from the receiver, we may reduce the analysis to a single (or a limited number of) mode(s) that would dominate the signal at the receiver [*Inan and Carpenter*, 1987]. In this case the phase change $\Delta\phi$ resulting from a localized (within the horizontal scale d), differential reduction in the ionospheric reflection height Δh for a single mode analysis can be expressed as [see *Inan and Carpenter*, 1987]

$$\frac{\Delta\phi}{d\Delta h} \cong -6.4\cdot 10^{-3}\ \mathrm{grad/km^2}$$

where an estimation of both d and Δh can be obtained from a model of interaction of tsunami-driven gravity waves with ionosphere.

In the model developed by *Rozhnoi et al*. [2012], a gravity wave, propagating through the nonisothermal atmosphere (that includes wind and molecular diffusion of heat and momentum), can dissipate at altitude of about 100 km, giving rise to an enhancement of the neutral temperature [*Pertsev and Shalimov*, 1996]. This results in a subsequent decrease in the temperature gradient with height and an increase in the turbulent diffusion coefficient which increases the vertical transport of NO molecules from the region of their active formation (100–120 km). This is accompanied by a subsequent increase in the electron concentration in the lower ionosphere through a chain of chemical reactions [see, for example, *Brasseur and Solomon*, 1984]. The increase in the electron density can cause localized ionospheric perturbations along the signal path leading to amplitude and phase variations. Now taking the characteristic vertical scale of NO redistribution to be comparable with the height scale H, and the horizontal scale is an order of a gravity wave wavelength λ_w, that is $d\sim\lambda_w$, $\Delta h\sim H$, we choose $\lambda_w \sim 300$ km, $H \sim 5$ km as representative values and obtain from the last expression an estimation for the phase anomaly of $\Delta\phi\sim 10°$. This result is of the order of measured in our experiment.

Finally, we note that the ionospheric perturbation may represent actually a wave train rather than a single wave in which case a real horizontal scale of the perturbation in the ionosphere can be larger than one wavelength (see observations of tsunami-driven gravity waves propagating in the airglow layer after the Tohoku earthquake [*Makela et al*., 2011]). If it is a few times larger, say, 3–5 wavelengths, this brings our phase anomaly estimation to agreement with our observations.

Some peculiarities of the observed effect that distinguish it from the previous one [*Rozhnoi et al*., 2012] should be mentioned here. In contrast to the previous examples (in analysis of Kuril 2006 and Tohoku 2011 tsunamis), the first or main tsunami in the current investigation propagated along the NPM-PTK path during local day so that we cannot observe the response of the lower ionosphere to the first tsunami using our VLF technique. However, the ionospheric effect produced by this tsunami was observed in the upper ionosphere using TEC detection by GPS satellites [*Galvan et al*., 2011].

The new point discussed in the present paper is that we observed a second tsunami and its ionospheric effects which have been missed in the previous observations in the upper ionosphere. The second wave was not caught by any numerical modeling either. Nevertheless, we confirmed the presence of the second tsunami by both our DARTs measurements and ionospheric measurements.

In conclusion, we have found observational evidence of variations in VLF signal measurements that are associated with the Chile tsunamis of 27 February 2010. Ionospheric effects displayed in the phase and amplitude perturbations of VLF signal appear to be caused by the tsunami-driven internal gravity waves. These gravity wave patterns revealed in spectral characteristics of the ionospheric disturbances within the VLF path sensitivity zone between Hawaii and Japan correlate in time, space, and wave properties with tsunamis recorded by DARTs in the same region after the Chile event.

Acknowledgments

We thank George Mungov (NOAA, NGDC, Boulder, CO) for providing us with the retrieved high-resolution DART data and Artem Loskutov (Institute of Marine Geology and Geophysics FEB RAS, Yuzhno-Sakhalinsk) for modeling. The work was supported by joint United Kingdom-Russia project under grant 13-05-92602 KO_a and under grant RFBR 14-05-00099.

Alan Rodger thanks David Galvan and an anonymous reviewer for their assistance in evaluating this paper.

References

Artru, J., V. Ducic, H. Kanamori, P. Lognonne, and M. Murakami (2005), Ionospheric detection of gravity waves induced by tsunamis, *Geophys. J. Int.*, *160*, 840–848, doi:10.1111/j.1365-246X.2005.02552.x.

Brasseur, G., and S. Solomon (1984), *Aeronomy of the Middle Atmosphere: Chemistry and Physics of the Stratosphere and Mesosphere*, 414 pp., D. Reidel Publ. Co., Dordrecht, Netherlands.

Coïsson, P., G. Occhipinti, P. Lognonné, J.-P. Molinié, and L. M. Rolland (2011), Tsunami signature in the ionosphere: A simulation of OTH radar observations, *Radio Sci.*, *46*, RS0D20, doi:10.1029/2010RS004603.

Dziewonski, A., S. Bloch, and M. Landisman (1969), A technique for the analysis of transient seismic signals, *Bull. Seismol. Soc. Am.*, *59*, 427–444.

Galvan, D. A., A. Komjathy, M. P. Hickey, and A. J. Mannucci (2011), The 2009 Samoa and 2010 Chile tsunamis as observed in the ionosphere using GPS total electron content, *J. Geophys. Res.*, *116*, A06318, doi:10.1029/2010JA016204.

Hickey, M. P., G. Schubert, and R. L. Walterscheid (2009), The propagation of tsunami-driven gravity waves into the thermosphere and ionosphere, *J. Geophys. Res.*, *114*, A08304, doi:10.1029/2009JA014105.

Hines, C. O. (1972), Gravity waves in the atmosphere, *Nature*, *239*, 73–78.
Inan, U. S., and D. L. Carpenter (1987), Lightning-induced electron precipitation events observed at L ~ 2.4 as phase and amplitude perturbations on subionospheric VLF signals, *J. Geophys. Res.*, *92*, 3293–3303, doi:10.1029/JA092iA04p03293.
Lander A. V., A. L. Levshin, V. F. Pisarenko, and G. A. Pogrebinsky (1973), About spectral-time analysis of oscillations, [in Russian], *Vichislitelnaya seimologia*, *6*, 3–27.
Levin, B., and M. Nosov (2009), *Physics of Tsunamis*, 327 pp., Springer, Berlin, Heidelberg, New York.
Mai, C.-L., and J.-F. Kiang (2009), Modeling of ionospheric perturbation by 2004 Sumatra tsunami, *Radio Sci.*, *44*, RS3011, doi:10.1029/2008RS004060.
Makela, J., et al. (2011), Imaging and modeling the ionospheric airglow response over Hawaii to the tsunami generated by the Tohoku earthquake of 11 March 2011, *Gephys. Res. Lett.*, *38*, L00G02, doi:10.1029/2011GL047860.
Mungov, G., M. Eblé, and R. Bouchard (2013), DART® tsunameter retrospective and real-time data: A reflection on 10 years of processing in support of tsunami research and operations, *Pure Appl. Geophys.*, *170*(9–10), 1369–1384, doi:10.1007/s00024-012-0477-5.
Najita, K., P. Weaver, and P. Yuen (1974), A tsunami warning system using an ionospheric technique, *Proc. IEEE*, *62*(5), 563–567.
Occhipinti, G., P. Lognonné, E. A. Kherani, and H. Hébert (2006), Three dimensional waveform modeling of ionospheric signature induced by the 2004 Sumatra tsunami, *Geophys. Res. Lett.*, *33*, L20104, doi:10.1029/2006GL026865.
Occhipinti, G., A. Kherani, and P. Lognonné (2008), Geomagnetic dependence of ionospheric disturbances induced by tsunamigenic internal gravity waves, *Geophys. J. Int.*, *173*(3), 753–765, doi:10.1111/j.1365-246X.2008.03760.
Peltier, W. R., and C. O. Hines (1976), On the possible detection of tsunamis by a monitoring of the ionosphere, *J. Geophys. Res.*, *81*, 1995–2000, doi:10.1029/JC081i012p01995.
Pertsev, N. N., and S. L. Shalimov (1996), The generation of atmospheric gravity waves in a seismically active region and their effect on the ionosphere, *Geomagn. Aeron. Engl. Transl.*, *36*, 223–227.
Rabinovich, A. B., R. Candella, and R. E. Thomson (2011), Energy decay of the 2004 Sumatra tsunami in the world ocean, *Pure Appl. Geophys.*, *168*(11), 1919–1950, doi:10.1007/s00024-01-0279-1.
Rabinovich, A. B., R. N. Candella, and R. E. Thomson (2013), The open ocean energy decay of three recent trans-Pacific tsunamis, *Geophys. Res. Lett.*, *40*, 3157–3162, doi:10.1002/grl.50625.
Rolland, L. M., G. Occhipinti, P. Lognonné, and A. Loevenbruck (2010), Ionospheric gravity waves detected offshore Hawaii after tsunamis, *Geophys. Res. Lett.*, *37*, L17101, doi:10.1029/2010GL044479.
Rozhnoi, A. A., M. S. Solovieva, O. A. Molchanov, M. Hayakawa, S. Maekawa, and P. F. Biagi (2006), Sensitivity of LF signal to global ionosphere and atmosphere perturbations in the network of stations, *Phys. Chem. Earth*, *31*, 409–415.
Rozhnoi, A., S. Shalimov, M. Solovieva, B. W. Levin, M. Hayakawa, and S. N. Walker (2012), Tsunami-induced phase and amplitude perturbations of subionospheric VLF signals, *J. Geophys. Res.*, *117*, A09313, doi:10.1029/2012JA017761.
Van Dorn, W. G. (1984), Some tsunami characteristics deducible from tide records, *J. Phys. Oceanogr.*, *14*, 353–363.
Van Dorn, W. G. (1987), Tide gage response to tsunamis. Part II: Other oceans and smaller seas, *J. Phys. Oceanogr.*, *17*, 1507–1516.
Wait, J. R. (1959), Diurnal change of ionospheric heights deduced from phase velocity measurements at VLF, *Proc. IRE*, *47*(5), 998.
Wait J. R., and K. P. Spies (1964), Characteristics of the earth-ionosphere waveguide for VLF radio waves, NBS Tech. Note 300, National Bureau of Standards, Boulder, Colo.